IMA Journal of Numerical Analysis (2022) **00**, 1–23
https://doi.org/10.1093/imanum/drac026

A C^0 finite element method for the biharmonic problem with Navier boundary conditions in a polygonal domain

Hengguang Li
Wayne State University, Department of Mathematics, Detroit, MI 48202, USA

Peimeng Yin*
Multiscale Methods and Dynamics Group, Computer Science and Mathematics Division, Oak Ridge National Laboratory, Oak Ridge, TN 37831, USA
*Corresponding author: yinp@ornl.gov

and

Zhimin Zhang
Wayne State University, Department of Mathematics, Detroit, MI 48202, USA and Beijing Computational Science Research Center, Beijing 100193, China

[Received on 16 December 2021; revised on 7 May 2022]

In this paper we study the biharmonic equation with Navier boundary conditions in a polygonal domain. In particular, we propose a method that effectively decouples the fourth-order problem as a system of Poisson equations. Our method differs from the naive mixed method that leads to two Poisson problems but only applies to convex domains; our decomposition involves a third Poisson equation to confine the solution in the correct function space, and therefore can be used in both convex and nonconvex domains. A C^0 finite element algorithm is in turn proposed to solve the resulting system. In addition, we derive optimal error estimates for the numerical solution on both quasi-uniform meshes and graded meshes. Numerical test results are presented to justify the theoretical findings.

Keywords: biharmonic equation; reentrant corner; mixed formulation; C^0 finite element method; optimal error estimates.

1. Introduction

Let $\Omega \subset \mathbb{R}^2$ be a polygonal domain. Consider the biharmonic problem

$$\Delta^2 u = f \quad \text{in } \Omega, \qquad u = 0 \quad \text{and} \quad \Delta u = 0 \quad \text{on } \partial\Omega. \tag{1.1}$$

† The work of Peimeng Yin is sponsored by the Office of Advanced Scientific Computing Research, US Department of Energy, and performed at the Oak Ridge National Laboratory, which is managed by UT-Battelle, LLC under Contract No. DE-AC05-00OR22725 with the US Department of Energy. The United States Government retains and the publisher, by accepting the article for publication, acknowledges that the United States Government retains a nonexclusive, paid-up, irrevocable, world-wide license to publish or reproduce the published form of this manuscript, or allow others to do so, for United States Government purposes. The Department of Energy will provide public access to these results of federally sponsored research in accordance with the DOE Public Access Plan (http://energy.gov/downloads/doe-public-access-plan).

The boundary conditions in (1.1) are referred to as the homogeneous Navier boundary conditions (Destuynder & Salaun, 1996; Rafetseder & Zulehner, 2018) that occur for example in the model for the static loading of a pure hinged thin plate. Equation (1.1) is a fourth-order elliptic equation for which a direct finite element approximation usually involves delicate construction of the finite element space (Argyris *et al.*, 1968; Brenner & Scott, 2002; Ciarlet Jr & He, 2003). An alternative approach is to use a mixed formulation to decompose the high-order problem into a system of equations that may be easier to solve. This approach is particularly appealing for the biharmonic problem (1.1) because the Navier boundary condition allows one to obtain two Poisson equations that are completely decoupled, which implies that a reasonable numerical solution should be achieved by merely applying a finite element Poisson solver to the mixed formulation. However, it has been observed (Nazarov & Sweers, 2007a; Zhang & Zhang, 2008; Gerasimov *et al.*, 2012; De Coster *et al.*, 2019) that the performance of this standard mixed method depends on the domain geometry. In a convex domain, the corresponding numerical approximations converge to the solution of equation (1.1), although the convergence rate may not be optimal. When the domain possesses reentrant corners, however, the result can be misleading: this mixed finite element formulation produces numerical solutions that may be converging to a wrong solution.

In this paper we propose a C^0 finite element algorithm for solving the biharmonic problem (1.1) and analyze its efficiency. In particular, we shall devise a modified mixed formulation to transform equation (1.1) into a system of three Poisson equations. This work is based on the observation that the aforementioned standard mixed formulation (decomposition into two Poisson equations) in fact defines a weak solution in a space larger than that for equation (1.1). This mismatch in function spaces does not affect the solution in a convex domain, while in a nonconvex domain it allows additional singular functions and therefore results in a solution different from that of equation (1.1) (known as the Sapongyan paradox; Nazarov & Plamenevsky, 1994; Zhang & Zhang, 2008). Our modified mixed formulation ensures that the associated solution is identical to the solution of (1.1) in both convex and nonconvex domains. This is accomplished by introducing an additional intermediate Poisson problem that confines the solution in the correct space.

To solve the proposed mixed formulation we present a numerical algorithm based on the piecewise linear C^0 finite element. Moreover, we derive the error analysis on the finite element approximations for both the auxiliary function w (see (2.11)) and the solution u. For the auxiliary function w, the error in the H^1 norm is standard and has a convergence rate $h^{\frac{\pi}{\omega}}$ on a quasi-uniform mesh, where ω is the interior angle of the reentrant corner; its L^2 error estimate can be obtained using a duality argument. For the solution u, the error in the H^1 norm is bounded by (i) the interpolation error of the solution u in H^1, (ii) the L^2 error for the auxiliary function w and (iii) the L^2 error for the solution ξ of the additional intermediate Poisson problem. We shall show that the proposed algorithm has the optimal H^1 convergence rate for the solution u on quasi-uniform meshes.

In addition, we present regularity estimates for the proposed system in a class of Kondratiev-type weighted spaces. Based on these regularity results, we in turn propose graded mesh refinement algorithms, such that the associated finite element methods recover the optimal convergence rate in the energy norm for the auxiliary function w even when w is singular. For clarity in the exposition, we adopt the linear C^0 finite element method in this paper with the assumption that the domain Ω has at most one reentrant corner. The cases involving high-order finite elements and multiple reentrant corners will be discussed in a forthcoming paper.

There is a rich literature on mixed finite element methods for the biharmonic problem, and most existing works are focused on the Dirichlet (clamped) boundary condition ($u = \partial_n u = 0$ on $\partial\Omega$). For example, Davini & Pitacco (2000) studied a mixed method, and in Zulehner (2015)

preconditioning techniques were investigated for the discrete system, both of which are based on the Ciarlet–Raviart formulation (Ciarlet & Raviart, 1974) for solving biharmonic problems with a clamped boundary condition. In addition, some other types of mixed variational formulations can be found in Gallistl (2017), Sweers (2009) for the clamped biharmonic problem. Notice that it is possible to extend the algorithm in Gallistl (2017) to solve equation (1.1). We also mention the related works Blum *et al.* (1980), De Coster *et al.* (2019) and the references therein for general regularity results for biharmonic problems, Bernardi *et al.* (1992) for a mixed spectral element method for the Navier–Stokes equations and Nazarov & Sweers (2007b) for Kirchhoff plate bending problems. In particular, De Coster *et al.* (2019) studied the Saponzhyan–Babushka paradox of the biharmonic problem with piecewise $C^{2,1}$ boundaries connecting at corners, and an augmented solution space is needed to correct the solution of the second-order system in the appropriate Sobolev-type space.

The method proposed in this paper effectively decouples the biharmonic problem (1.1) into a system of Poisson equations, whose solution is equivalent to that of the original problem in both convex and nonconvex domains. The C^0 finite element algorithm is simple, robust and effective in practical computations for problem (1.1). Our method can be further applied to cases involving multiple reentrant corners and high-order finite element approximations. Moreover, with suitable modifications, we expect to extend this algorithm to some other high-order problems, such as a class of fourth-order problems with low-order terms and sixth-order problems with similar boundary conditions. It is also reasonable to explore the extension of this work to fourth-order problems with nonlinear operators or other boundary conditions.

The rest of the paper is organized as follows. In Section 2, based on the general regularity theory for second-order elliptic equations (Kondrat'ev, 1967; Moussaoui, 1985; Grisvard, 1992; Kozlov *et al.*, 1997, 2001), especially Nazarov & Svirs (2007a), we review the weak solutions of the biharmonic problem (1.1) and the naive mixed formulation. In addition, we discuss the orthogonal space of the image of the operator $-\Delta$, which is one-dimensional, and identify a basis function in this space. Then we propose a modified mixed formulation and show the equivalence of its solution to the original biharmonic problem. In Section 3 we propose the finite element algorithm and obtain error estimates on quasi-uniform meshes for both the solution u and the auxiliary function w. In Section 4 we introduce a weighted Sobolev space and derive regularity estimates for the solution near the reentrant corner. Then we present the graded mesh algorithm and provide optimal error estimates on graded meshes. We report numerical test results in Section 5 to validate the theory.

Throughout the paper, the generic constant $C > 0$ in our estimates may be different at different occurrences. It will depend on the computational domain, but not on the functions involved nor on the mesh level in the finite element algorithms.

2. The biharmonic problem

2.1 *Well-posedness of the solution*

Denote by $H^m(\Omega)$, $m \geq 0$ the Sobolev space that consists of functions whose ith derivatives are square integrable for $0 \leq i \leq m$. Let $L^2(\Omega) := H^0(\Omega)$. Recall that $H_0^1(\Omega) \subset H^1(\Omega)$ is the subspace consisting of functions with zero trace on the boundary $\partial\Omega$. We shall denote the norm $\|\cdot\|_{L^2(\Omega)}$ by $\|\cdot\|$ when there is no ambiguity about the underlying domain. For $s > 0$, let $s = m + t$, where $m \in \mathbb{Z}_{\geq 0}$ and $0 < t < 1$. Recall that for $D \subseteq \mathbb{R}^d$, the fractional-order Sobolev space $H^s(D)$ consists of distributions v

in D satisfying

$$\|v\|^2_{H^s(D)} := \|v\|^2_{H^m(D)} + \sum_{|\alpha|=m} \int_D \int_D \frac{|\partial^\alpha v(x) - \partial^\alpha v(y)|^2}{|x-y|^{d+2t}} \mathrm{d}x\,\mathrm{d}y < \infty,$$

where $\alpha = (\alpha_1, \ldots, \alpha_d) \in \mathbb{Z}^d_{\geq 0}$ is a multi-index such that $\partial^\alpha = \partial^{\alpha_1}_{x_1} \cdots \partial^{\alpha_d}_{x_d}$ and $|\alpha| = \sum_{i=1}^d \alpha_i$. Let $\widetilde{H}^s(D)$ be the space of all v defined in D such that $\tilde{v} \in H^s(\mathbb{R}^d)$, where $\tilde{v}$ is the extension of v by zero outside D.

The following variational formulation for equation (1.1) can be obtained using integration by parts:

$$a(u,v) := \int_\Omega \Delta u \Delta v \,\mathrm{d}x = \int_\Omega fv \,\mathrm{d}x = (f,v) \quad \forall\, v \in H^2(\Omega) \cap H^1_0(\Omega). \tag{2.1}$$

For a function $v \in H^2(\Omega) \cap H^1_0(\Omega)$, applying the Poincaré-type inequality (Grisvard, 1992, Theorem 2.2.3) gives $\|\Delta v\|_{L^2(\Omega)} \geq C\|v\|_{H^2(\Omega)}$. Then by the Lax–Milgram theorem, equation (2.1) defines a unique weak solution $u \in H^2(\Omega) \cap H^1_0(\Omega)$ for any f in the dual space of $H^2(\Omega) \cap H^1_0(\Omega)$ (namely, $f \in \left(H^2(\Omega) \cap H^1_0(\Omega)\right)^*$). The regularity of the solution u depends on the given data f and the domain geometry (Blum *et al.*, 1980).

2.2 *The naive mixed formulation*

Intuitively, equation (1.1) can be decoupled into a system of two Poisson problems by introducing an auxiliary function w such that

$$\begin{cases} -\Delta w = f & \text{in } \Omega, \\ w = 0 & \text{on } \partial\Omega, \end{cases} \quad \text{and} \quad \begin{cases} -\Delta \bar{u} = w & \text{in } \Omega, \\ \bar{u} = 0 & \text{on } \partial\Omega, \end{cases} \tag{2.2}$$

where $(\bar{u}, w) \in H^1_0(\Omega) \times H^1_0(\Omega)$. We refer to (2.2) as the naive mixed formulation. Note that numerical solvers for the Poisson problems (2.2) are readily available, while numerical approximation of the fourth-order problem (1.1) is generally a much harder task. The mixed weak formulation of (2.2) is to find $\bar{u}, w \in H^1_0(\Omega)$ such that

$$A(w,\phi) = (f,\phi) \quad \forall\, \phi \in H^1_0(\Omega), \tag{2.3a}$$

$$A(\bar{u},\psi) = (w,\psi) \quad \forall\, \psi \in H^1_0(\Omega), \tag{2.3b}$$

where

$$A(\phi,\psi) = \int_\Omega \nabla\phi \cdot \nabla\psi \,\mathrm{d}x.$$

Given $f \in H^{-1}(\Omega) \subset \left(H^2(\Omega) \cap H^1_0(\Omega)\right)^*$, it is clear that the weak solutions $\bar{u}, w$ are well defined by (2.3) because they are solutions of decoupled Poisson problems (Evans, 1998). Since our goal is to solve the biharmonic problem (1.1), an important question is whether the solution u in (2.1) and the solution $\bar{u}$ in (2.3) are the same.

REMARK 2.1 For $f \in H^{-1}(\Omega)$, existing results suggest that under appropriate conditions, the solution $\bar{u}$ of system (2.3) is equivalent to the solution u of equation (2.1) in the sense that

$$u = \bar{u} \text{ in } H^2(\Omega) \cap H^1_0(\Omega).$$

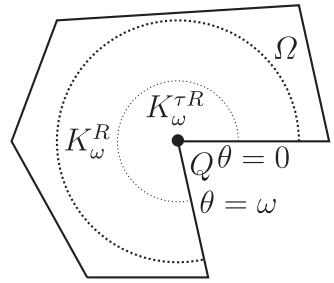

FIG. 1. Domain Ω containing a reentrant corner.

These conditions include (i) the domain Ω and the given data f being smooth, which can be verified by the regularity of these equations up to the domain boundary (Gilbarg & Trudinger, 1983; Li & Nistor, 2009), (ii) the polygonal domain Ω being convex (Zhang & Zhang, 2008). It is however pointed out that u is not always equivalent to $\bar{u}$ when the polygonal domain Ω has reentrant corners, which is known as the Sapongyan paradox (Nazarov & Plamenevsky, 1994; Zhang & Zhang, 2008). In this case, the numerical solution for (2.3) does not converge to the solution of the biharmonic problem (1.1). In the next subsection, we shall study the structure of the solution in the presence of a reentrant corner in order to design effective numerical algorithms for equation (1.1).

2.3 *Image of the Laplace operator and its orthogonal space*

From now on we assume the given function $f \in L^2(\Omega)$ in (1.1). In addition, assume that the polygonal domain Ω has a reentrant corner associated with the vertex Q and the corresponding interior angle $\omega \in (\pi, 2\pi)$. Without loss of generality, we set Q to be the origin. Let (r, θ) be polar coordinates centered at the vertex Q, such that ω is spanned by two half-lines $\theta = 0$ and $\theta = \omega$. Given $R > 0$ we identify a sector $K_\omega^R \subset \Omega$ with radius R as

$$K_\omega^R = \{(r\cos\theta, r\sin\theta) \in \Omega \mid 0 \le r \le R, 0 \le \theta \le \omega\}.$$

A sketch drawing of the domain Ω is shown in Fig. 1.

The mapping $-\Delta : H^2(\Omega) \cap H_0^1(\Omega) \to L^2(\Omega)$ is injective and has a closed range (Grisvard, 1992). Denote by $\mathcal{M}$ the image of this mapping and by $\mathcal{M}^\perp$ its orthogonal complement. Then it follows that $\mathcal{M} \oplus \mathcal{M}^\perp = L^2(\Omega)$. Therefore, if $w \in \mathcal{M}$ in (2.3), we have equivalent solutions $u = \bar{u}$ in $H^2(\Omega) \cap H_0^1(\Omega)$. When the domain Ω is convex, one has $\mathcal{M} = L^2(\Omega)$; namely, the solution of the Poisson equation with Dirichlet boundary condition is always in $H^2(\Omega)$ when $f \in L^2(\Omega)$. Thus, in a convex domain the condition $w \in H_0^1(\Omega) \subset \mathcal{M}$ holds, and therefore the solutions u and $\bar{u}$ are equivalent. However, if Ω contains reentrant corners, $\mathcal{M}$ is a strict subset of $L^2(\Omega)$ and in general $w \notin \mathcal{M}$. Consequently, the solution in (2.2) $\bar{u} \notin H^2(\Omega)$ and it is different from the solution of (1.1) $u \in H^2(\Omega) \cap H_0^1(\Omega)$. Fortunately, the space $\mathcal{M}^\perp$ is finite-dimensional and it is possible to identify its basis.

We first introduce an L^2 function in domain Ω in the following way.

DEFINITION 2.2 Given the parameters $\tau \in (0, 1)$ and R such that $K_\omega^R \subset \Omega$, we define an L^2 function in Ω,

$$\xi(r, \theta; \tau, R) := s^-(r, \theta; \tau, R) + \zeta(r, \theta; \tau, R), \tag{2.4}$$

where

$$s^-(r,\theta;\tau,R) = \eta(r;\tau,R) r^{-\frac{\pi}{\omega}} \sin\left(\frac{\pi}{\omega}\theta\right) \in L^2(\Omega), \tag{2.5}$$

with cut-off function $\eta(r;\tau,R) \in C^\infty(\Omega)$ satisfying $\eta(r;\tau,R) = 1$ for $0 \le r \le \tau R$ and $\eta(r;\tau,R) = 0$ for $r > R$, and $\zeta \in H_0^1(\Omega)$ satisfies

$$-\Delta\zeta = \Delta s^- \text{ in } \Omega, \qquad \zeta = 0 \text{ on } \partial\Omega. \tag{2.6}$$

From (2.5) we see that $s^- \in C^\infty(\Omega \setminus K_\omega^\delta)$ for any $\delta > 0$ and $s^- = 0$ for $(r\cos\theta, r\sin\theta) \in \Omega \setminus K_\omega^R$. Moreover, $\Delta s^- = 0$ if $r < \tau R$ or $r > R$.

REMARK 2.3 The function ξ and its variants have been used for solving the Poisson equation with singularities. For example, using a fixed coefficient $\tau = \frac{1}{2}$, ξ was utilized in Blum & Dobrowolski (1981), Cai & Kim (2001), and another version of ξ without the cut-off function was analyzed in Lions & Magenes (1972), Ciarlet & Raviart (1974). When solving the biharmonic problem (1.1), we shall see in the next section that all these versions of ξ lead to similar finite element algorithms. However, the value of τ can affect the value of s^- in Algorithm 3.1, which will be elaborated on later.

Denote the ith side of $\partial\Omega$ by $\bar{\Gamma}_i$, where Γ_i is open. For the function ξ defined in (2.4), we introduce the maximal extension of the Laplace operator in $L^2(\Omega)$:

$$D(\Delta, L^2(\Omega)) := \{v \in L^2(\Omega) : \ \Delta v \in L^2(\Omega)\}.$$

For a function v, let $\gamma_i v$ be the restriction of v to Γ_i. Then the mapping

$$v \mapsto \gamma_i v$$

that is defined for $v \in H^2(\Omega)$ has a unique continuous extension from $D(\Delta, L^2(\Omega))$ into $\widetilde{H}^{-\frac{1}{2}}(\Gamma_i)$ (Grisvard, 1992, Theorem 1.5.2), where $\widetilde{H}^{-\frac{1}{2}}(\Gamma_i)$ is the dual space of $\widetilde{H}^{\frac{1}{2}}(\Gamma_i)$ that is defined at the beginning of Section 2. Then we have the following properties of ξ.

LEMMA 2.4 For a given $\eta \in C^\infty(\Omega)$ as defined in Definition 2.2, the function $\xi \in D(\Delta, L^2(\Omega))$ is uniquely defined and satisfies

$$-\Delta\xi = 0 \text{ in } \Omega, \qquad \xi = 0 \text{ on } \partial\Omega. \tag{2.7}$$

In addition, ξ depends on the domain Ω, but not on τ or R. Namely, for any τ_1, τ_2 and R_1, R_2 satisfying $0 < \delta < \min\{\tau_1 R_1, \tau_2 R_2\}$, it follows that

$$\xi(r,\theta) := \xi(r,\theta;\tau_1,R_1) = \xi(r,\theta;\tau_2,R_2). \tag{2.8}$$

Proof. The condition in (2.7) follows from Grisvard (1992, Lemma 2.3.6). We proceed to prove (2.8). For $0 < \delta < \min\{\tau_1 R_1, \tau_2 R_2\}$, we have $K_\omega^\delta \subset K_\omega^{\tau_1 R_1} \cap K_\omega^{\tau_2 R_2} \subset \Omega$. By (2.5) we have

$$s^-(r,\theta;\tau_1,R_1) - s^-(r,\theta;\tau_2,R_2) = 0, \quad (r,\theta) \in K_\omega^\delta.$$

Recall that $s^-(r,\theta;\tau_i,R_i) \in C^\infty(\Omega \setminus K_\omega^\delta)$; then it follows that

$$s^-(r,\theta;\tau_1,R_1) - s^-(r,\theta;\tau_2,R_2) \in C^\infty(\Omega).$$

Since $\zeta(r,\theta;\tau_i,R_i) \in H_0^1(\Omega)$, we have

$$\begin{aligned}\tilde{\xi} &:= \xi(r,\theta;\tau_1,R_1) - \xi(r,\theta;\tau_2,R_2)\\ &= \zeta(r,\theta;\tau_1,R_1) - \zeta(r,\theta;\tau_2,R_2) + \big(s^-(r,\theta;\tau_1,R_1) - s^-(r,\theta;\tau_2,R_2)\big) \in H_0^1(\Omega).\end{aligned}$$

From (2.7) we have

$$\Delta\tilde{\xi} = \Delta\xi(r,\theta;\tau_1,R_1) - \Delta\xi(r,\theta;\tau_2,R_2) = 0 \text{ in } \Omega, \qquad \tilde{\xi} = 0 \text{ on } \partial\Omega.$$

By the Lax–Milgram theorem, we have $\tilde{\xi} = 0$, and thus (2.8) holds. □

From now on we shall write $\xi(r,\theta)$ instead of $\xi(r,\theta;\tau,R)$, since it is independent of τ and R. We also notice that $\xi(r,\theta) \not\equiv 0$, because otherwise we have $s^- = -\zeta \in H_0^1(\Omega)$, which contradicts the fact that $s^- \notin H_0^1(\Omega)$.

REMARK 2.5 It is clear that $\xi \in D(\Delta, L^2(\Omega))$ is an $L^2(\Omega)$ solution of the boundary value problem (2.7). It is interesting to note that different from the $H^1(\Omega)$ solution, the $L^2(\Omega)$ solution to problem (2.7) is not unique. For example, there are at least two $L^2(\Omega)$ solutions for (2.7), one is $\xi = 0$, which is also the unique $H^1(\Omega)$ solution, and the other is $\xi \not\equiv 0$ as defined in (2.4). Note that the boundary condition in (2.7) is defined in the trace sense, namely $\xi \in \widetilde{H}^{-\frac{1}{2}}(\Gamma_i)$ on each side.

Now we are ready to describe the subspace $\mathcal{M}^\perp$. For the dimension of $\mathcal{M}^\perp$, we have the following results from Grisvard (1992, Theorem 2.3.7).

LEMMA 2.6 The dimension of $\mathcal{M}^\perp$ is equal to the cardinality of the set $\{\lambda_k : 0 < \lambda_k < 1\}$ for $k \geq 1$, namely

$$\dim(\mathcal{M}^\perp) = \operatorname{card}\{\lambda_k : 0 < \lambda_k < 1\},$$

with λ_k^2 being the eigenvalues of the one-dimensional problem

$$-\partial_{\theta\theta}\phi_k = \lambda_k^2\phi_k \quad \text{in } (0,\omega), \qquad \phi(0) = \phi(\omega) = 0.$$

For $k \geq 1$, it is clear that when $\lambda_k > 0$,

$$\lambda_k = \frac{k\pi}{\omega}, \quad \phi_k = \sqrt{\frac{2}{\omega}}\sin\left(\frac{k\pi}{\omega}\theta\right). \tag{2.9}$$

Hence, for the domain Ω with one reentrant corner, $\mathcal{M}^\perp$ satisfies the following lemma.

LEMMA 2.7 The dimension of $\mathcal{M}^\perp$ is $\dim(\mathcal{M}^\perp) = 1$ and $\mathcal{M}^\perp = \operatorname{span}\{\xi(r,\theta)\}$, where $\xi(r,\theta)$ is the L^2 function defined in (2.4).

By Lemma 2.7, any $w \in L^2(\Omega)$ can be uniquely expressed as

$$w = w_{\mathcal{M}} + c\xi,$$

where $w_{\mathcal{M}} = w - c\xi \in \mathcal{M}$ and the coefficient

$$c = \frac{(w,\xi) - (w_{\mathcal{M}},\xi)}{\|\xi\|^2} = \frac{(w,\xi)}{\|\xi\|^2}. \tag{2.10}$$

2.4 *The modified mixed formulation*

Based on the discussion above, we propose a modified mixed formulation for (1.1),

$$\begin{cases} -\Delta w = f & \text{in } \Omega, \\ w = 0 & \text{on } \partial\Omega, \end{cases} \quad \text{and} \quad \begin{cases} -\Delta \tilde{u} = w - c\xi & \text{in } \Omega, \\ \tilde{u} = 0 & \text{on } \partial\Omega, \end{cases} \tag{2.11}$$

where ξ is given in (2.4) and the coefficient c is shown in (2.10). The corresponding modified mixed weak formulation for (2.11) is to find $\tilde{u}, w \in H_0^1(\Omega)$ such that

$$A(w,\phi) = (f,\phi), \tag{2.12a}$$

$$A(\tilde{u},\psi) = (w - c\xi,\psi), \tag{2.12b}$$

for any $\phi, \psi \in H_0^1(\Omega)$.

Then we have the following result for the modified mixed formulation.

THEOREM 2.8 Given $f \in L^2(\Omega)$, let $\tilde{u}$ be the solution of the modified mixed weak formulation (2.12) and let u be the solution of the weak formulation (2.1). Then it follows that $\tilde{u} \in H^2(\Omega) \cap H_0^1(\Omega)$ and $u = \tilde{u}$.

Proof. Since $f \in L^2(\Omega)$ we have $w \in H_0^1(\Omega) \subset L^2(\Omega)$. Thus it follows that $w - c\xi \in \mathcal{M}$, which implies $\tilde{u} \in H^2(\Omega) \cap H_0^1(\Omega)$. Then (2.12b) becomes

$$-(\Delta\tilde{u},\psi) = (w - c\xi,\psi) \quad \forall\, \psi \in H_0^1(\Omega). \tag{2.13}$$

Note $\Delta\tilde{u} \in L^2(\Omega)$. Then following the density argument, (2.13) leads to

$$-(\Delta\tilde{u},\psi) = (w - c\xi,\psi), \quad \forall\, \psi \in L^2(\Omega).$$

Thus, for any $\phi \in H^2(\Omega) \cap H_0^1(\Omega)$, we have $\Delta\phi \in L^2(\Omega)$ and therefore

$$(\Delta\tilde{u},\Delta\phi) = (w - c\xi, -\Delta\phi). \tag{2.14}$$

Since $\xi \in L^2(\Omega)$, $\Delta\xi = 0 \in L^2(\Omega)$, using Green's theorem (Grisvard, 1992, Theorem 1.5.3) and (2.7), we have that $(\xi,\Delta\phi) = 0$. Then the right-hand side of (2.14) becomes

$$(w - c\xi, -\Delta\phi) = A(w,\phi) + (c\xi,\Delta\phi) = A(w,\phi) = (f,\phi),$$

where the last equation is based on (2.12a). Hence we have obtained that $\tilde{u} \in H^2(\Omega) \cap H_0^1(\Omega)$ satisfies

$$(\Delta\tilde{u}, \Delta\phi) = (f, \phi) \quad \forall\, \phi \in H^2(\Omega) \cap H_0^1(\Omega).$$

This is the same equation as (2.1) that defines u. Consequently, $\tilde{u} = u \in H^2(\Omega) \cap H_0^1(\Omega)$ and we have completed the proof. □

Therefore, by Theorem 2.8, the solution u of the biharmonic problem (1.1) satisfies

$$\begin{cases} -\Delta w = f & \text{in } \Omega, \\ w = 0 & \text{on } \partial\Omega, \end{cases} \quad \text{and} \quad \begin{cases} -\Delta u = w - c\xi & \text{in } \Omega, \\ u = 0 & \text{on } \partial\Omega. \end{cases} \tag{2.15}$$

The corresponding weak formulation is to find $u, w \in H_0^1(\Omega)$ such that for any $\phi, \psi \in H_0^1(\Omega)$,

$$A(w, \phi) = (f, \phi), \tag{2.16a}$$

$$A(u, \psi) = (w - c\xi, \psi), \tag{2.16b}$$

where c is given in (2.10).

In addition, we have the following regularity result.

LEMMA 2.9 Given $f \in L^2(\Omega)$, for w, u in the modified mixed formulation (2.15), it follows that

$$\|w\|_{H^1(\Omega)} \leq C\|f\|, \tag{2.17a}$$

$$\|u\|_{H^2(\Omega)} \leq C\|f\|. \tag{2.17b}$$

Proof. Estimate (2.17a) is a direct consequence of the fact that the Laplace operator is an isomorphism between $H_0^1(\Omega)$ and $H^{-1}(\Omega)$ and $\|f\|_{H^{-1}(\Omega)} \leq C\|f\|$. By the Lax–Milgram theorem for (2.1), we have that Δ is also an isomorphism from $H^2(\Omega) \cap H_0^1(\Omega)$ to its dual. Therefore, estimate (2.17b) follows from this observation and Theorem 2.8. □

3. The finite element method

In this section we propose a linear C^0 finite element method solving the biharmonic problem (1.1). Then we derive the finite element error analysis for the solution u to show that our method will achieve the optimal convergence rate especially when the domain is nonconvex.

3.1 *The finite element algorithm*

Let $\mathcal{T}_n$ be a triangulation of Ω with shape-regular triangles and let $S_n \subset H_0^1(\Omega)$ be the C^0 Lagrange finite element space associated with $\mathcal{T}_n$,

$$S_n(\mathcal{T}) := \{v \in C^0(\Omega) \cap H_0^1(\Omega) : \ v|_T \in P_1 \ \forall\, T \in \mathcal{T}_n\}, \tag{3.1}$$

where P_1 is the space of polynomials of degree no more than 1. Then we proceed to propose the finite element algorithm.

ALGORITHM 3.1 We define the finite element solution of the biharmonic problem (1.1) by utilizing the decoupling in (2.16) as follows.

- Step 1. Find the finite element solution $w_n \in S_n$ of the Poisson equation
$$A(w_n, \phi) = (f, \phi) \qquad \forall\, \phi \in S_n. \tag{3.2}$$
- Step 2. With s^- defined in (2.5), we compute the finite element solution $\zeta_n \in S_n$ of the Poisson equation
$$A(\zeta_n, \phi) = (\Delta s^-, \phi) \qquad \forall\, \phi \in S_n, \tag{3.3}$$
and set $\xi_n = \zeta_n + s^-$.
- Step 3. Find the coefficient $c_n \in \mathbb{R}$ such that
$$\int_\Omega (w_n - c_n\xi_n)\xi_n \,\mathrm{d}x = 0,$$
or equivalently, we compute the coefficient
$$c_n = \frac{(w_n, \xi_n)}{\|\xi_n\|^2} = \frac{(w_n, \zeta_n) + (w_n, s^-)}{\|s^-\|^2 + \|\zeta_n\|^2 + 2(\zeta_n, s^-)}. \tag{3.4}$$
- Step 4. Find the finite element solution $u_n \in S_n$ of the Poisson equation
$$A(u_n, \psi) = (w_n - c_n\xi_n, \psi) \qquad \forall\, \psi \in S_n. \tag{3.5}$$

REMARK 3.2 The function s^- in (2.5) exists only in the presence of a reentrant corner. When the domain is convex, we set $s^- = 0$ and Algorithm 3.1 reduces to the naive mixed finite element algorithm for equation (1.1). According to (3.3), $\zeta_n \in S_n$, while $\xi_n \in L^2(\Omega)$ but $\xi_n \notin S_n$. In addition, the finite element approximations in Algorithm 3.1 are well defined based on the Lax–Milgram theorem.

REMARK 3.3 All the integrals in Algorithm 3.1 can be effectively approximated by quadrature rules except for the term $\|s^-\|^2 = \int_{K_\omega^R} (s^-)^2 \,\mathrm{d}x$ in (3.4), due to the lack of regularity in the integrand. Namely, $s^- \in H^\beta(K_\omega^R)$ with $\beta < 1 - \frac{\pi}{\omega}$. Only evaluating $\|s^-\|^2$ by quadrature rules may destroy the convergence rate of the proposed algorithm. In practice, we evaluate $\|s^-\|^2$ in the following way:

$$\begin{aligned}
\|s^-\|^2 &= \int_{K_\omega^R} (s^-)^2 \,\mathrm{d}x = \int_{K_\omega^{\tau R}} (s^-)^2 \,\mathrm{d}x + \int_{K_\omega^R \setminus K_\omega^{\tau R}} (s^-)^2 \,\mathrm{d}x \\
&= \int_0^\omega \left(\int_0^{\tau R} + \int_{\tau R}^R \right) \left(\eta(r;\tau,R) r^{-\frac{\pi}{\omega}} \sin\left(\frac{\pi}{\omega}\theta\right) \right)^2 r \,\mathrm{d}r \,\mathrm{d}\theta \\
&= \int_0^\omega \int_0^{\tau R} r^{1-\frac{2\pi}{\omega}} \sin^2\left(\frac{\pi}{\omega}\theta\right) \mathrm{d}r \,\mathrm{d}\theta + \int_0^\omega \int_{\tau R}^R \eta^2(r;\tau,R) r^{1-\frac{2\pi}{\omega}} \sin^2\left(\frac{\pi}{\omega}\theta\right) \mathrm{d}r \,\mathrm{d}\theta \\
&= \frac{\omega(\tau R)^{2-\frac{2\pi}{\omega}}}{4 - \frac{4\pi}{\omega}} + \frac{\omega}{2} \int_{\tau R}^R \eta^2(r;\tau,R) r^{1-\frac{2\pi}{\omega}} \,\mathrm{d}r,
\end{aligned} \tag{3.6}$$

where the one-dimensional definite integral in the last equation can be calculated directly or evaluated by a quadrature rule in one dimension. The computational technique (3.6) is accurate, and at the same time can significantly reduce the computational cost in evaluating the integral.

3.2 *Optimal error estimates on quasi-uniform meshes*

Suppose that the mesh $\mathcal{T}_n$ consists of quasi-uniform triangles with size h. Recall the interpolation error estimate on $\mathcal{T}_n$ (Ciarlet Jr & He, 2003) for any $v \in H^l(\Omega)$, $l > 1$:

$$\|v - v_I\|_{H^m(\Omega)} \leq Ch^{l-m}\|v\|_{H^l(\Omega)}, \tag{3.7}$$

where $m = 0, 1$ and $v_I \in S_n$ represents the nodal interpolation of v. For the Poisson equations (2.6) and (2.15) in the polygonal domain with a reentrant corner, given $f \in L^2(\Omega)$, it is well known that $w, \zeta \in H^\alpha(\Omega)$ with $\alpha < 1 + \frac{\pi}{\omega}$ (see e.g., Grisvard, 1985, 1992). Recall the finite element approximations w_n and ζ_n in (3.2) and (3.3), respectively. Due to the lack of regularity, the standard error estimate (Ciarlet Jr & He, 2003) yields

$$\|w - w_n\|_{H^1(\Omega)} \leq Ch^{\alpha-1}\|w\|_{H^\alpha(\Omega)}, \quad \|\zeta - \zeta_n\|_{H^1(\Omega)} \leq Ch^{\alpha-1}\|\zeta\|_{H^\alpha(\Omega)}. \tag{3.8}$$

Note that $\xi - \xi_n = \zeta - \zeta_n \in H^\alpha(\Omega)$, and thus

$$\|\xi - \xi_n\|_{H^1(\Omega)} \leq Ch^{\alpha-1}\|\zeta\|_{H^\alpha(\Omega)}. \tag{3.9}$$

In addition, we have the following L^2 error analysis.

LEMMA 3.4 Given w_n and ξ_n in Algorithm 3.1, we have

$$\|w - w_n\| \leq Ch^{2\alpha-2}\|w\|_{H^\alpha(\Omega)}, \quad \|\xi - \xi_n\| \leq Ch^{2\alpha-2}\|\zeta\|_{H^\alpha(\Omega)}. \tag{3.10}$$

Proof. We only prove the error estimate for $w - w_n$, and the estimate for $\xi - \xi_n (= \zeta - \zeta_n)$ can be obtained similarly. Consider the Poisson problem

$$-\Delta v = g \text{ in } \Omega, \quad v = 0 \text{ on } \partial\Omega, \tag{3.11}$$

where $g \in L^2(\Omega)$. By the Aubin–Nitsche lemma in Ciarlet Jr & He (2003, Theorem 3.2.4), we have

$$\|w - w_n\| \leq C\|w - w_n\|_{H^1(\Omega)} \sup_{g \neq 0 \in L^2(\Omega)} \left(\frac{\inf_{\phi \in S_n} \|v - \phi\|_{H^1(\Omega)}}{\|g\|} \right). \tag{3.12}$$

For $\alpha \in \left(1, 1 + \frac{\pi}{\omega}\right) \subset (1, 2)$, the regularity result (Grisvard, 1985, 1992) gives $\|v\|_{H^\alpha(\Omega)} \leq C_\alpha\|g\|_{H^{\alpha-2}} \leq C\|g\|$. Then we have

$$\inf_{\phi \in S_n} \|v - \phi\|_{H^1(\Omega)} \leq \|v - v_I\|_{H^1(\Omega)} \leq Ch^{\alpha-1}\|v\|_{H^\alpha(\Omega)} \leq Ch^{\alpha-1}\|g\|. \tag{3.13}$$

Combining the estimates in (3.13), (3.12) and (3.8), we have completed the proof. □

Next we carry out the error estimate for the finite element approximation u_n in (3.5).

THEOREM 3.5 Let $u_n \in S_n$ be the finite element approximation to (3.5), and u be the solution to the biharmonic problem (2.1). Then it follows that

$$\|u - u_n\|_{H^1(\Omega)} \leq Ch.$$

Proof. For any $\phi \in S_n$, based on (2.16b) and (3.5), we have

$$\begin{aligned} A(u, \phi) =& (w, \phi) - c(\xi, \phi), \\ A(u_n, \phi) =& (w_n, \phi) - c_n(\xi_n, \phi). \end{aligned}$$

Taking the difference of the two equations above, we have

$$\begin{aligned} A(u - u_n, \phi) =& (w - w_n, \phi) + c_n(\xi_n, \phi) - c(\xi, \phi) \\ =& (w - w_n, \phi) + c_n(\xi_n - \xi, \phi) + (c_n - c)(\xi, \phi). \end{aligned} \tag{3.14}$$

Let $u_I \in S_n$ be the nodal interpolation of u. Set $\epsilon = u_I - u$, $e = u_I - u_n$ and take $\phi = e$ in (3.14). We have

$$A(e, e) = A(\epsilon, e) + (w - w_n, e) + c_n(\xi_n - \xi, e) + (c_n - c)(\xi, e).$$

Thus, we have

$$\|e\|^2_{H^1(\Omega)} \leq C \left(\|\epsilon\|_{H^1(\Omega)} + \|w - w_n\|_{H^{-1}(\Omega)} + |c_n| \|\xi_n - \xi\|_{H^{-1}(\Omega)} + |c - c_n| \|\xi\|_{H^{-1}(\Omega)} \right) \|e\|_{H^1(\Omega)}.$$

Using the triangle inequality and the inequality above we have

$$\begin{aligned} \|u - u_n\|_{H^1(\Omega)} \leq & \|e\|_{H^1(\Omega)} + \|\epsilon\|_{H^1(\Omega)} \\ \leq & C \left(\|\epsilon\|_{H^1(\Omega)} + \|w - w_n\|_{H^{-1}(\Omega)} + |c_n| \|\xi_n - \xi\|_{H^{-1}(\Omega)} + |c - c_n| \|\xi\|_{H^{-1}(\Omega)} \right) \\ \leq & C \left(\|\epsilon\|_{H^1(\Omega)} + \|w - w_n\| + |c_n| \|\xi_n - \xi\| + |c - c_n| \|\xi\| \right). \end{aligned} \tag{3.15}$$

The last inequality is based on the fact that the H^{-1} norm of an L^2 function is bounded by its L^2 norm. We shall estimate every term in (3.15). Recall the solution $u \in H^2(\Omega)$. By the interpolation error estimate (3.7),

$$\|\epsilon\|_{H^1(\Omega)} = \|u - u_I\|_{H^1(\Omega)} \leq Ch \|u\|_{H^2(\Omega)}. \tag{3.16}$$

Recall the angle of the reentrant corner $\omega \in (\pi, 2\pi)$. Thus, choosing $\alpha = 3/2 < 1 + \frac{\pi}{\omega}$ in (3.10), we have

$$\|w - w_n\| \leq Ch, \quad \|\xi - \xi_n\| \leq Ch. \tag{3.17}$$

To obtain the error estimate for the third term in (3.15), we still need to show that $|c_n|$ is uniformly bounded. Recall that $\xi \not\equiv 0$ depends only on the domain Ω, and so is

$$\|\xi\| > 0. \tag{3.18}$$

Moreover, when $h \le h_0 := \min\{1, \sqrt[2\alpha-2]{\frac{\|\xi\|}{2C\|\xi\|_{H^\alpha(\Omega)}}}\}$, it follows from (3.10) that

$$\frac{1}{2}\|\xi\| \le \|\xi_n\| \le \frac{3}{2}\|\xi\|. \tag{3.19}$$

By setting $\phi = w_n$ in (3.2) and applying the Poincaré inequality, we obtain

$$\|w_n\| \le C\|w_n\|_{H^1(\Omega)} \le C\|f\|. \tag{3.20}$$

By (3.4), (3.19) and (3.20), we have the uniform boundedness,

$$|c_n| \le \frac{\|w_n\|}{\|\xi_n\|} \le C\|f\|, \tag{3.21}$$

where C is a constant depending on Ω. Subtracting (3.4) from (2.10) we obtain

$$c - c_n = \frac{(w - w_n, \xi)}{\|\xi\|^2} + \frac{(\xi - \xi_n, w_n)}{\|\xi_n\|^2} + \frac{\|\xi_n\|^2 - \|\xi\|^2}{\|\xi\|^2\|\xi_n\|^2}(w_n, \xi).$$

By the uniform boundedness for terms in (3.18), (3.19), (3.20) and the estimates in (3.17), we have for the last term in (3.15),

$$|c - c_n|\|\xi\| \le \|w - w_n\| + \frac{(\|\xi_n\| + 2\|\xi\|)\|w_n\|}{\|\xi_n\|^2}\|\xi - \xi_n\| \le Ch. \tag{3.22}$$

Then the proof is completed by plugging (3.16), (3.21), (3.22) and (3.17) into (3.15). □

REMARK 3.6 The error estimate in Theorem 3.5 shows that the proposed finite element algorithm (Algorithm 3.1) produces numerical solutions that converge to the solution of the biharmonic problem (1.1) when the domain Ω is nonconvex. In the case that Ω is convex, Algorithm 3.1 reduces to the naive mixed finite element algorithm for equation (1.1) that has proven to be effective (Zhang & Zhang, 2008). Therefore, Algorithm 3.1 approximates the target equation in both convex and nonconvex domains. On a quasi-uniform mesh, the convergence is first order (optimal) for u in the H^1 norm (Theorem 3.5) and suboptimal (3.8) for the auxiliary function w in the H^1 norm. In Algorithm 3.1, one shall solve three Poisson problems. Given the availability of fast Poisson solvers, Algorithm 3.1 is a relatively easy and cost effective alternative to existing algorithms solving (1.1).

4. Optimal error estimates on graded meshes

The numerical approximations from Algorithm 3.1 are optimal for u but only sub-optimal for w. It is largely due to the lack of regularity for w. Recall that for $f \in L^2(\Omega)$, w is merely in $H^\alpha(\Omega)$ for

$\alpha < 1 + \frac{\pi}{\omega}$. In this section we study system (2.16) in a class of weighted Sobolev spaces and in turn propose graded triangulations that lead to numerical solutions converging at the optimal rate to both u and w.

4.1 *Regularity in weighted Sobolev spaces*

We now introduce the Kondratiev-type weighted spaces for the analysis of system (2.16).

DEFINITION 4.1 [Weighted Sobolev spaces] Recall that Q is the vertex at the reentrant corner. Let $r(x)$ be the distance from x to Q. For $a \in \mathbb{R}$, $m \geq 0$ and $G \subset \Omega$, we define the weighted Sobolev space

$$\mathcal{K}_a^m(G) := \{v,\ r^{|\alpha|-a}\partial^\alpha v \in L^2(G)\ \forall\, |\alpha| \leq m\},$$

where the multi-index $\alpha = (\alpha_1, \alpha_2) \in \mathbb{Z}^2_{\geq 0}$, $|\alpha| = \alpha_1 + \alpha_2$ and $\partial^\alpha = \partial_x^{\alpha_1}\partial_y^{\alpha_2}$. The $\mathcal{K}_a^m(G)$ norm for v is defined by

$$\|v\|_{\mathcal{K}_a^m(G)} = \left(\sum_{|\alpha|\leq m}\int_G |r^{|\alpha|-a}\partial^\alpha v|^2 \mathrm{d}x\right)^{\frac{1}{2}}.$$

REMARK 4.2 According to Definition 4.1, in the region that is away from the reentrant corner, the weighted space $\mathcal{K}_a^m$ is equivalent to the Sobolev space H^m. In the neighborhood of Q, the space $\mathcal{K}_a^m$ is the same Kondratiev space (Kondrat'ev, 1967; Grisvard, 1985; Dauge, 1988). Recall the first equation in (2.15) that defines w. In the Dirichlet Poisson problem, the reentrant corner can give rise to singularities in w, such that $w \notin H^2(\Omega)$. It is the reason that the finite element approximation to w on a quasi-uniform mesh is not optimal. The singularity in w is however local and concentrates in the neighborhood of Q. Involving a proper weight function, the space $\mathcal{K}_a^m$ may allow more singular functions and is an important tool for analyzing corner singularities.

In the weighted Sobolev space we have the following regularity result for system (2.16).

LEMMA 4.3 Assume $a < \frac{\pi}{\omega}$ and $f \in L^2(\Omega)$. Recall ζ in (2.6). Then it follows that

$$\|\zeta\|_{\mathcal{K}^2_{a+1}(\Omega)} \leq C\|\Delta s^-\|.$$

In addition, recall w in (2.15). Then we have

$$\|w\|_{\mathcal{K}^2_{a+1}(\Omega)} \leq C\|f\|.$$

Proof. Since $\Delta s^-, f \in L^2(\Omega) \subset \mathcal{K}^0_{a-1}(\Omega)$, the desired estimates follow by applying Li & Nicaise (2018, Theorem 3.3) to equations (2.6) and (2.15). □

4.2 *Graded meshes*

We now present the construction of graded meshes to improve the convergence rate of the numerical approximation from Algorithm 3.1.

ALGORITHM 4.4 [Graded refinements] Let $\mathcal{T}$ be a triangulation of Ω with shape-regular triangles. Recall that Q is the vertex of Ω at the reentrant corner. It is clear that Q is also a vertex in the triangulation

FIG. 2. The new node on an edge pq (left – right): $p \neq Q$ and $q \neq Q$ (midpoint); $p = Q$ ($|pr| = \kappa|pq|$, $\kappa < 0.5$).

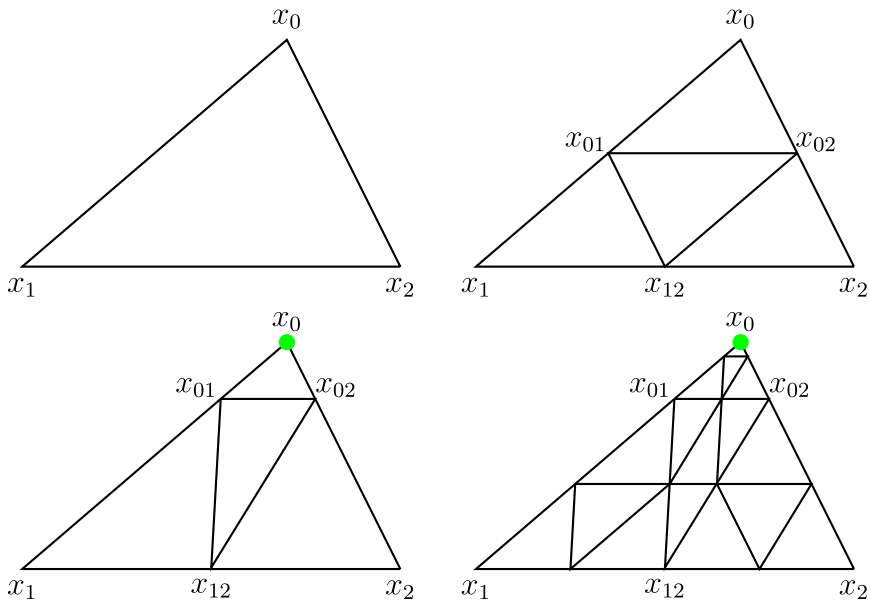

FIG. 3. Refinement of a triangle $\triangle x_0x_1x_2$. First row: (left to right): the initial triangle and the midpoint refinement; second row: two consecutive graded refinements toward $x_0 = Q$, ($\kappa < 0.5$).

$\mathcal{T}$. Let pq be an edge in the triangulation $\mathcal{T}$ with p and q as the endpoints. Then, in a graded refinement, a new node r on pq is produced according to the following conditions:

1. (Neither p or q coincides with Q.) We choose r as the midpoint ($|pr| = |qr|$).
2. (p coincides with Q.) We choose r such that $|pr| = \kappa|pq|$, where $\kappa \in (0, 0.5)$ is a parameter that will be specified later. See Fig. 2 for example.

Then the graded refinement, denoted by $\kappa(\mathcal{T})$, proceeds as follows. For each triangle $T \in \mathcal{T}$, a new node is generated on each edge of as described above. Then T is decomposed into four small triangles by connecting these new nodes (Fig. 3). Given an initial mesh $\mathcal{T}_0$ satisfying the condition above, the associated family of graded meshes $\{\mathcal{T}_n, n \geq 0\}$ is defined recursively $\mathcal{T}_{n+1} = \kappa(\mathcal{T}_n)$.

Given a grading parameter κ, Algorithm 4.4 produces smaller elements near Q for better approximation of a singular solution. It is an explicit construction of graded meshes based on recursive refinements. See also Apel *et al.* (1996), Băcuţă *et al.* (2005), Krendl *et al.* (2016), Li & Nicaise (2018) and the references therein for more discussions on the graded mesh. Note that after n refinements, the number of triangles in the mesh $\mathcal{T}_n$ is $\mathcal{O}(4^n)$.

4.3 *Optimal error estimates on graded meshes*

In the rest of this section we shall show that with a proper selection of the grading parameter κ, the proposed numerical solutions u_n and w_n converge to the solutions u and w of (2.15) at the optimal rate on graded meshes. Recall the finite element space S_n in (3.1) associated with the graded mesh $\mathcal{T}_n$.

We first recall the following interpolation error estimates (Apel *et al.*, 1996; Li & Nicaise, 2018) for functions in the weighted space.

LEMMA 4.5 Let $0 < a < \frac{\pi}{\omega}$ and choose the grading parameter $\kappa = 2^{-1/a}$. Define $h := 2^{-n}$. Then for any $v \in \mathcal{K}^2_{a+1}(\Omega)$, it follows that

$$\|v - v_I\|_{H^1(\Omega)} \leq Ch\|v\|_{\mathcal{K}^2_{a+1}(\Omega)},$$

where v_I is the nodal interpolation of v associated with $\mathcal{T}_n$.

Now we proceed to derive the optimal error estimates of $w - w_n$ and $\xi - \xi_n$ on graded meshes.

LEMMA 4.6 Let $0 < a < \frac{\pi}{\omega}$ and choose $\kappa = 2^{-1/a}$. Then for the approximations w_n and ξ_n defined in (3.2) and (3.3), it follows that

$$\|w - w_n\|_{H^1(\Omega)} \leq Ch\|w\|_{\mathcal{K}^2_{a+1}(\Omega)}, \quad \|w - w_n\| \leq Ch^2\|w\|_{\mathcal{K}^2_{a+1}(\Omega)},$$
$$\|\xi - \xi_n\|_{H^1(\Omega)} \leq Ch\|\zeta\|_{\mathcal{K}^2_{a+1}(\Omega)}, \quad \|\xi - \xi_n\| \leq Ch^2\|\zeta\|_{\mathcal{K}^2_{a+1}(\Omega)},$$

where $h := 2^{-n}$.

Proof. The H^1 error estimates for $w - w_n$ and $\zeta - \zeta_n$ follow from the standard H^1 error estimates on graded meshes (Apel *et al.*, 1996). We only prove the L^2 error estimates for $w - w_n$ and the estimates for $\zeta - \zeta_n$ will follow similarly. Applying the Aubin–Nitsche lemma to (3.11) again, we have

$$\|w - w_n\| \leq C\|w - w_n\|_{H^1(\Omega)} \sup_{g \neq 0 \in L^2(\Omega)} \left(\frac{\inf_{\phi \in S_n} \|v - \phi\|_{H^1(\Omega)}}{\|g\|} \right). \tag{4.1}$$

Based on the regularity estimate in Lemma 4.3, the function v in (3.11) satisfies

$$\|v\|_{\mathcal{K}^2_{a+1}(\Omega)} \leq C\|g\|.$$

Together with Lemma 4.5, we have

$$\inf_{\phi \in S_n} \|v - \phi\|_{H^1(\Omega)} \leq \|v - v_I\|_{H^1(\Omega)} \leq Ch\|v\|_{\mathcal{K}^2_{a+1}(\Omega)} \leq Ch\|g\|, \tag{4.2}$$

where v_I is the nodal interpolation of v associated with $\mathcal{T}_n$. Plugging (4.2) into (4.1) leads to the desired error estimate for $\|w - w_n\|$.

The H^1 and L^2 error estimates of $\xi - \xi_n$ follow by the relationship $\xi - \xi_n = \zeta - \zeta_n$. □

REMARK 4.7 Note that the error estimates for $w-w_n$, $\zeta-\zeta_n$ follow from the standard H^1 error estimate on both uniform meshes (Ciarlet Jr & He, 2003) and graded meshes (Apel *et al.*, 1996). However, the H^1 and L^2 error estimates of $\xi-\xi_n$ are obtained based on the relationship $\xi-\xi_n=\zeta-\zeta_n$.

We conclude this section with the H^1 error estimate for the solution u of the biharmonic problem (1.1) on graded meshes.

THEOREM 4.8 Let $\mathcal{T}_n$ be the graded mesh with the grading parameter $0<\kappa<\frac{1}{2}$. Let u_n be the finite element approximation to u that is defined in Algorithm 3.1. Then it follows that

$$\|u-u_n\|_{H^1(\Omega)}\leq Ch,$$

where $h:=2^{-n}$.

Proof. Let u_I be the nodal interpolation of u associated with $\mathcal{T}_n$. Similar to the analysis in Theorem 3.5 on quasi-uniform meshes, we have

$$\|u-u_n\|_{H^1(\Omega)}\leq C\left(\|u-u_I\|_{H^1(\Omega)}+\|w-w_n\|+\frac{\|w_n\|}{\|\xi_n\|}\|\xi_n-\xi\|+|c-c_n|\|\xi\|_{H^{-1}(\Omega)}\right). \tag{4.3}$$

For $0<\kappa<\frac{1}{2}$, the following interpolation error still holds:

$$\|u-u_I\|_{H^1(\Omega)}\leq Ch\|u\|_{H^2(\Omega)}. \tag{4.4}$$

Thus, the proof is completed by combining the estimates in (4.3), (4.4), (3.22) and the L^2 error estimates for $w-w_n$ and $\xi-\xi_n$ in (3.10). □

REMARK 4.9 According to Theorems 3.5 and 4.8, the numerical solution u_n in Algorithm 3.1 approximates the solution u of the biharmonic problem in the optimal H^1 convergence rate on quasi-uniform meshes and also on graded meshes defined in Algorithm 4.4. In addition, a proper graded mesh can improve the effectiveness in approximating the auxiliary function w in (2.15). In particular, selecting the grading parameter κ as in Lemma 4.6, the proposed finite element solution w_n converges to w in both H^1 and L^2 norms with the optimal rate on graded meshes. Nonetheless, the numerical approximations u_n and w_n from Algorithm 3.1 converge to u and w in both convex and nonconvex domains. The graded mesh can improve the convergence rate but does not make divergent numerical solutions convergent. We also point out that when high-order finite element methods are used in Algorithm 3.1, new graded meshes are needed to recover the optimal H^1 convergence rate for both u and w. We shall study these cases in future works.

5. Numerical illustrations

In this section we present numerical test results to validate our theoretical predictions for the proposed finite element method solving equation (1.1). Since the solutions u, w in (2.15) are unknown, we use the numerical convergence rate

$$\mathcal{R}=\log_2\frac{|v_j-v_{j-1}|_{H^1(\Omega)}}{|v_{j+1}-v_j|_{H^1(\Omega)}} \tag{5.1}$$

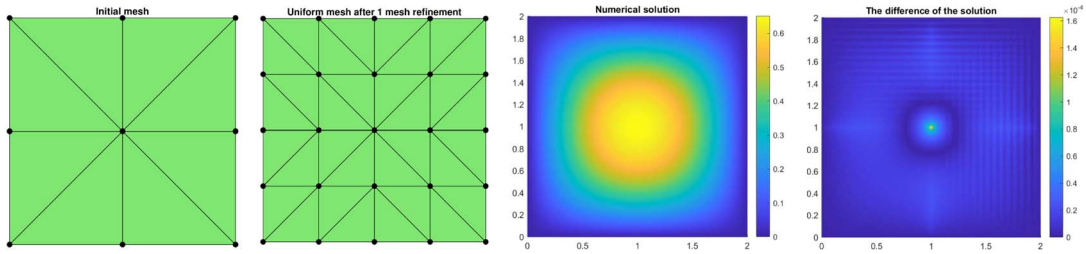

FIG. 4. The square domain (Example 5.1): (a) the initial mesh; (b) the mesh after one refinement; (c): the solution u_7 from Algorithm 3.1; (d) $|u_R - u_7|$.

TABLE 1 *H^1 Convergence history of the P_1 elements in Example 5.1 on uniform meshes*

	$j=3$	$j=4$	$j=5$	$j=6$
$\mathcal{R}$ for u_j	0.96	0.99	1.00	1.00
$\mathcal{R}$ for w_j	0.96	0.99	1.00	1.00

as an indicator of the actual convergence rate. Here v_j denotes the finite element solution on the mesh $\mathcal{T}_j$ obtained after j refinements of the initial triangulation $\mathcal{T}_0$. It can be either u_j or w_j depending on the underlying Poisson problem. In particular, suppose the actual convergence rate is $\|v-v_j\|_{H^1(\Omega)} = \mathcal{O}(h^\beta)$ for $\beta > 0$. Then for the P_1 finite element method, the rate in (5.1) is a good approximation of the exponent β as the level of refinements j increases (Li *et al.*, 2010).

We shall use the solution of the C^0 interior penalty discontinuous Galerkin (C^0-IPDG) method (Brenner, 2012) programmed in the software FEniCS (Alnæs *et al.*, 2015) as a reference solution. More specifically, we use the C^0-IPDG method based on P_2 polynomials with the penalty parameter $\eta = 24$. The reference solution is computed on the mesh after seven mesh refinements of the given initial mesh and is denoted by u_R. Since the C^0-IPDG method leads to numerical solutions converging to the solution u regardless of the convexity of the domain, we can use u_R as a good approximation of u.

EXAMPLE 5.1 (A convex domain). We consider problem (1.1) with $f = 10$ in the square domain $\Omega = (0,2)^2$. Since all the vertices have angles less than π, Algorithm 3.1 coincides with the naive mixed finite element method based on the formulations in (2.3).

We solve this problem using Algorithm 3.1 on uniform meshes obtained by midpoint refinements with the initial mesh given in Fig. 4(a). The finite element solution u_7 and the difference $|u_R - u_7|$ are shown in Figs 4(c) and 4(d), respectively. The convergence rates (5.1) for u_j and w_j on a sequence of uniform meshes are shown in Table 1. We see that the solution of the mixed finite element method converges to the solution of the biharmonic equation (1.1) and the optimal convergence rate ($\mathcal{R} = 1$) is achieved for both the numerical solution u_j and the auxiliary finite element solution w_j. This is consistent with our expectation (Remark 2.1) for the problem in a convex domain.

EXAMPLE 5.2 (A nonconvex domain). In this example, we investigate the convergence of Algorithm 3.1 by considering equation (1.1) with $f = 1$ in an L-shaped domain $\Omega = \Omega_0 \setminus \Omega_1$ with $\Omega_0 = (-2,2)^2$

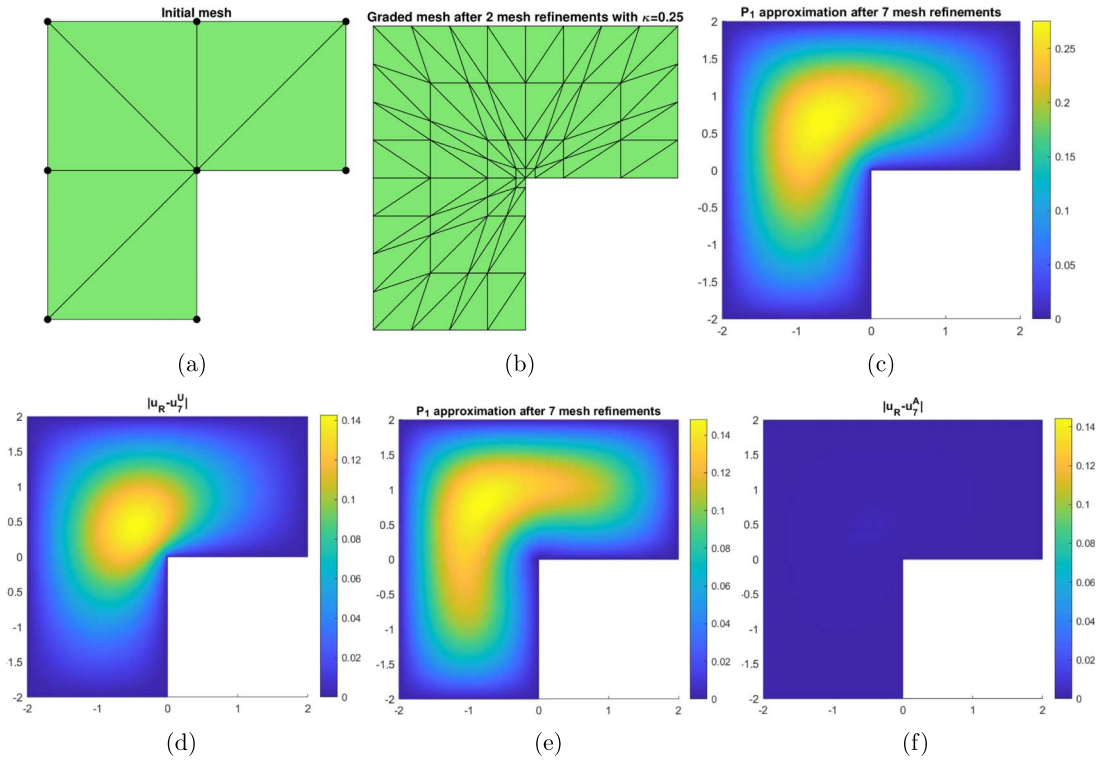

FIG. 5. The L-shaped domain (Example 5.2): (a) the initial mesh; (b) the graded mesh after two refinements; (c) the solution u_7^U of the naive mixed method; (d) the difference $|u_R - u_7^U|$; (e) the solution u_7^A from Algorithm 3.1; (f) the difference $|u_R - u_7^A|$.

and $\Omega_1 = (0,2) \times (-2,0)$. We use the following cut-off function in the algorithm:

$$\eta(r;\tau,R) = \begin{cases} 0 & \text{if } r \geq R, \\ 1 & \text{if } r \leq \tau R, \\ \frac{1}{2} - \frac{15}{16}\left(\frac{2r}{R(1-\tau)} - \frac{1+\tau}{1-\tau}\right) + \frac{5}{8}\left(\frac{2r}{R(1-\tau)} - \frac{1+\tau}{1-\tau}\right)^3 - \frac{3}{16}\left(\frac{2r}{R(1-\tau)} - \frac{1+\tau}{1-\tau}\right)^5 & \text{otherwise,} \end{cases}$$

where $R = \frac{9}{5}, \tau = \frac{1}{8}$.

In the first test, we solve equation (1.1) in the L-shaped domain using quasi-uniform meshes and compare the performances of Algorithm 3.1 and the naive mixed finite element algorithm based on formulation (2.3). On $\mathcal{T}_j$ we denote the numerical solutions from Algorithm 3.1 by u_j^A and w_j^A, and denote the numerical solutions from the naive mixed finite element algorithm by u_j^U and w_j^U. The initial mesh is shown in Fig. 5(a). In Table 2 we display the errors ($u_R - u_j^U$ and $u_R - u_j^A$) in the L^∞ norm between the finite element solutions and the reference solution u_R. In addition, the differences $|u_R - u_7^U|$ and $|u_R - u_7^A|$ are presented in Figs 5(d) and 5(f). From these results we see that the solution u_j^A from Algorithm 3.1 converges to the actual solution, while the solution u_j^U of the naive mixed finite element algorithm does not converge to the solution of the biharmonic equation (1.1) as the meshes are refined. These

TABLE 2 *The L^∞ error in the L-shaped domain on quasi-uniform meshes*

	$j=3$	$j=4$	$j=5$	$j=6$
$\|u_R - u_j^U\|_{L^\infty(\Omega)}$	1.28014e−01	1.37318e−01	1.41309e−01	1.42525e−01
$\|u_R - u_j^A\|_{L^\infty(\Omega)}$	1.58074e−02	7.84320e−03	3.20391e−03	1.20794e−03

TABLE 3 *Numerical convergence rates $\mathcal{R}$ for u_j^U and w_j^U in the L-shaped domain*

$\kappa \backslash j$	u_j^U					w_j^U				
	$j=5$	$j=6$	$j=7$	$j=8$	$j=9$	$j=5$	$j=6$	$j=7$	$j=8$	$j=9$
$\kappa=0.1$	0.95	0.98	0.99	1.00	1.00	0.95	0.98	0.99	1.00	1.00
$\kappa=0.2$	0.96	0.99	1.00	1.00	1.00	0.96	0.99	0.99	1.00	1.00
$\kappa=0.3$	0.97	0.98	0.99	0.99	0.99	0.96	0.98	0.99	0.99	0.99
$\kappa=0.4$	0.94	0.94	0.94	0.93	0.93	0.94	0.95	0.95	0.94	0.94
$\kappa=0.5$	0.86	0.82	0.78	0.75	0.72	0.87	0.84	0.80	0.77	0.74

observations are closely aligned with our theoretical predictions in Remark 3.6. Namely, Algorithm 3.1 gives rise to convergent numerical solutions in both convex and nonconvex domains, while the naive mixed method is applicable only for convex domains.

For the naive mixed finite element method, although the solution u_j^U does not converge to the solution of (1.1), we notice that both u_j^U and w_j^U, $j \geq 0$ are converging sequences. The numerical convergence rate $\mathcal{R}$ (5.1) for u_j^U and w_j^U on a sequence of graded meshes (including quasi-uniform meshes) is reported in Table 3. In the table we observe that u_j^U and w_j^U have similar convergence rates: $\mathcal{R} < 1$ on quasi-uniform meshes and on the graded meshes with $\kappa = 0.4$; and $\mathcal{R} = 1$ on graded meshes with $\kappa \leq 0.3$. These results indicate that the naive mixed finite element solution u_j^U converges to the solution $\bar{u}$ of (2.2) in $H^1(\Omega)$. Recall however that $\bar{u} \neq u$ when the domain has reentrant corners.

In the last test, we examine the convergence rates of the finite element solution u_j^A and the auxiliary finite element solution w_j^A from Algorithm 3.1 on a sequence of graded meshes (including quasi-uniform meshes). The H^1 convergence rates (5.1) for the finite element solutions u_j^A and w_j^A are reported in Table 4. For u_j^A, the optimal convergence rate ($\mathcal{R} = 1$) is achieved on all meshes with $\kappa \in (0, 0.5]$. For the auxiliary solution w_j^A, we observe that the convergence rate is not optimal on quasi-uniform meshes and on the graded meshes with $\kappa = 0.4$; and the optimal convergence rate $\mathcal{R} = 1$ is obtained on graded meshes when $\kappa \leq 0.3$. These numerical results justify the theory (Theorems 3.5, 4.8 and Lemma 4.6) developed early in this paper. Namely, the numerical solution u_j^A converges to u at the optimal rate on quasi-uniform meshes and on graded meshes, while w_j^A will converge to w in the optimal rate when $\kappa < 2^{-\frac{\omega}{\pi}} = 2^{-\frac{3}{2}} \approx 0.354$. For $\kappa > 2^{-\frac{3}{2}}$ ($\kappa = 0.4, 0.5$ in Table 4), w_j^A shall converge to w at a reduced rate due to the fact that w is singular near the reentrant corner ($w \notin H^2(\Omega)$ and $w \in H^\alpha(\Omega)$ for $\alpha < 1 + \frac{2}{3} \approx 1.667$ see; (3.8)).

EXAMPLE 5.3 In this example we compare the CPU time and the memory usage of the proposed finite element algorithm (Algorithm 3.1) with those of the C^0-IPDG method programmed in FEniCS. More specifically, the tests are based on these two algorithms/methods for biharmonic problems in

TABLE 4 *H^1 convergence history in the L-shaped domain on graded meshes*

$\kappa \backslash j$	u_j^A					w_j^A				
	$j=5$	$j=6$	$j=7$	$j=8$	$j=9$	$j=5$	$j=6$	$j=7$	$j=8$	$j=9$
$\kappa=0.1$	0.95	0.98	0.99	1.00	1.00	0.95	0.98	0.99	1.00	1.00
$\kappa=0.2$	0.95	0.99	1.00	1.00	1.00	0.96	0.99	0.99	1.00	1.00
$\kappa=0.3$	0.97	0.99	1.00	1.00	1.00	0.96	0.98	0.99	0.99	0.99
$\kappa=0.4$	0.98	0.99	1.00	1.00	1.00	0.94	0.95	0.95	0.94	0.94
$\kappa=0.5$	0.97	0.99	0.99	1.00	1.00	0.87	0.84	0.80	0.77	0.74

TABLE 5 *The CPU time (in seconds) of Algorithm 3.1 and the C^0-IPDG method in FEniCS. ('—' represents running out of memory)*

method$\backslash j$	Example 5.1					Example 5.2				
	$j=5$	$j=6$	$j=7$	$j=8$	$j=9$	$j=5$	$j=6$	$j=7$	$j=8$	$j=9$
C^0-IPDG	0.65	4.38	31.85	279.19	—	0.56	3.30	24.12	189.15	—
Algorithm 3.1	0.07	0.28	1.21	5.08	24.2	0.12	0.46	1.82	8.15	35.60

TABLE 6 *The memory usage (in GB) of Algorithm 3.1 and the C^0-IPDG method in FEniCS. ('—' represents running out of memory)*

method$\backslash j$	Example 5.1					Example 5.2				
	$j=5$	$j=6$	$j=7$	$j=8$	$j=9$	$j=5$	$j=6$	$j=7$	$j=8$	$j=9$
C^0-IPDG	0.14	0.34	1.28	5.74	—	0.12	0.25	0.91	4.04	—
Algorithm 3.1	<0.01	0.01	0.02	0.28	1.26	<0.01	<0.01	0.01	0.16	0.94

both Examples 5.1 and 5.2 on quasi-uniform meshes. The results of the CPU time (in seconds) of both algorithms/methods are shown in Table 5. Here, the CPU time does not include the mesh generation time since we assume they are the same. The results of the memory usage (in GB) are shown in Table 6. In this example, all results are tested on Ubuntu 20.04 with 16 GB memory and Intel Core^{TM} i7-6600U processors.

From Table 5 we find that given the same triangulation, the implementation of the proposed finite element algorithm (Algorithm 3.1) can be much faster than that of the C^0-IPDG method, due to the availability of fast Poisson solvers. At the same time, Table 6 indicates that Algorithm 3.1 uses less memory compared with the C^0-IPDG method. These results demonstrate the efficacy of our algorithm for solving the biharmonic problem (1.1).

Acknowledgements

The authors wish to express many thanks to anonymous reviewers who helped to improve the results and presentation.

Funding

National Science Foundation (DMS-1819041 to H.L.); Wayne State University Faculty Competition for Postdoctoral Fellows Award (to H.L.); National Natural Science Foundation of China (NSFC 11871092 and NASF U1930402 to Z.Z.).

Conflict of interest

The authors declare that they have no known competing financial interests or personal relationships that could have appeared to influence the work reported in this paper.

References

Alnæs, M., Blechta, J., Hake, J., Johansson, A., Kehlet, B., Logg, A., Richardson, C., Ring, J., Rognes, M. & Wells, G. (2015) The FEniCS project version 1.5. *Arch. Numer. Softw.*, **3**.

Apel, T., Sändig, A.-M. & Whiteman, J. (1996) Graded mesh refinement and error estimates for finite element solutions of elliptic boundary value problems in non-smooth domains. *Math. Methods Appl. Sci.*, **19**, 63–85.

Argyris, J. H., Fried, I. & Scharpf, D. W. (1968) The TUBA family of plate elements for the matrix displacement method. *Aeronaut. J.*, **72**, 701–709.

Băcuţă, C., Nistor, V. & Zikatanov, L. T. (2005) Improving the rate of convergence of 'high order finite elements' on polygons and domains with cusps. *Numer. Math.*, **100**, 165–184.

Bernardi, C., Girault, V. & Maday, Y. (1992) Mixed spectral element approximation of the Navier–Stokes equations in the stream-function and vorticity formulation. *IMA J. Numer. Anal.*, **12**, 565–608.

Blum, H. & Dobrowolski, M. (1981) Une méthode d'éléments finis pour la résolution des problèmes elliptiques dans des ouverts avec coins. *C. R. Acad. Sci. Paris, Sér. I*, **293**, 99–101.

Blum, H., Rannacher, R. & Leis, R. (1980) On the boundary value problem of the biharmonic operator on domains with angular corners. *Math. Methods Appl. Sci.*, **2**, 556–581.

Brenner, S. C. (2012) C^0 interior penalty methods. *Frontiers in Numerical Analysis–Durham 2010*. Lect. Notes Comput. Sci. Eng. 85 (J. Blowey & M. Jensen eds). Berlin, Heidelberg: Springer, pp. 79–147.

Brenner, S. C. & Scott, L. R. (2002) *The Mathematical Theory of Finite Element Methods, 2nd edn.* Texts in Applied Mathematics, vol. 15. New York: Springer.

Cai, Z. & Kim, S. (2001) A finite element method using singular functions for the Poisson equation: corner singularities. *SIAM J. Numer. Anal.*, **39**, 286–299.

Ciarlet Jr, P. & He, J. (2003) The singular complement method for 2D scalar problems. *C. R. Math.*, **336**, 353–358.

Ciarlet, P. G. (1978) *The Finite Element Method for Elliptic Problems*. Studies in Mathematics and Its Applications, vol. 4. Amsterdam: North-Holland.

Ciarlet, P. G. & Raviart, P.-A. (1974) A mixed finite element method for the biharmonic equation. *Mathematical Aspects of Finite Elements in Partial Differential Equations (Proc. Sympos., Math. Res. Center, Univ. Wisconsin, Madison, Wis., 1974)*. New York: Academic Press, pp. 125–145. Publication No. 33, 1974.

Dauge, M. (1988) *Elliptic Boundary Value Problems on Corner Domains*. Lecture Notes in Mathematics, vol. 1341. Berlin: Springer.

Davini, C. & Pitacco, I. (2000) An unconstrained mixed method for the biharmonic problem. *SIAM J. Numer. Anal.*, **38**, 820–836.

De Coster, C., Nicaise, S. & Sweers, G. (2019) Comparing variational methods for the hinged Kirchhoff plate with corners. *Math. Nachr.*, **292**, 2574–2601.

Destuynder, P. & Salaun, M. (1996) *Mathematical Analysis of Thin Plate Models*. Mathématiques & Applications (Berlin), vol. 24. Berlin: Springer.

Evans, L. (1998) *Partial Differential Equations*. Graduate Studies in Mathematics, vol. 19. Providence, RI: American Mathematical Society.

Gallistl, D. (2017) Stable splitting of polyharmonic operators by generalized stokes systems. *Math. Comp.*, **86**, 2555–2577.

Gerasimov, T., Stylianou, A. & Sweers, G. (2012) Corners give problems when decoupling fourth order equations into second order systems. *SIAM J. Numer. Anal.*, **50**, 1604–1623.

Gilbarg, D. & Trudinger, N. S. (1983) *Elliptic Partial Differential Equations of Second Order*. Berlin: Springer.

Grisvard, P. (1985) *Elliptic Problems in Nonsmooth Domains*. Boston: Pitman.

Grisvard, P. (1992) *Singularities in Boundary Value Problems*. Research Notes in Applied Mathematics, vol. 22. New York: Springer.

Kondrat'ev, V. A. (1967) Boundary value problems for elliptic equations in domains with conical or angular points. *Trudy Moskov. Mat. Obšč.*, **16**, 209–292.

Kozlov, V., Maz'ya, V. & Rossmann, J. (1997) *Elliptic Boundary Value Problems in Domains with Point Singularities*. Mathematical Surveys and Monographs, vol. 52. Providence, RI: American Mathematical Society.

Kozlov, V., Maz'ya, V. & Rossmann, J. (2001) *Spectral Problems Associated with Corner Singularities of Solutions to Elliptic Equations*. Mathematical Surveys and Monographs, vol. 85. Providence, RI: American Mathematical Society.

Krendl, W., Rafetseder, K. & Zulehner, W. (2016) A decomposition result for biharmonic problems and the Hellan–Herrmann–Johnson method. *Electron. Trans. Numer. Anal.*, **45**, 257–282.

Li, H., Mazzucato, A. & Nistor, V. (2010) Analysis of the finite element method for transmission/mixed boundary value problems on general polygonal domains. *Electron. Trans. Numer. Anal.*, **37**, 41–69.

Li, H. & Nicaise, S. (2018) Regularity and a priori error analysis on anisotropic meshes of a Dirichlet problem in polyhedral domains. *Numer. Math.*, **139**, 47–92.

Li, H. & Nistor, V. (2009) Analysis of a modified Schrödinger operator in 2D: regularity, index, and FEM. *J. Comput. Appl. Math.*, **224**, 320–338.

Lions, J. L. & Magenes, E. (1972) *Non-Homogeneous Boundary Value Problems and Applications I, III*. New York: Springer.

Moussaoui, M. A. (1985) Sur l'approximation des solutions du problème de Dirichlet dans un ouvert avec coins. *Singularities and Constructive Methods for Their Treatment*. Berlin, Heidelberg, pp. 199–206.

Nazarov S. & Plamenevsky, B. A. (1994) *Elliptic Problems in Domains with Piecewise Smooth Boundaries*. Berlin/New York: de Gruyter.

Nazarov, S. A. & Sweers, G. H. (2007a) A boundary-value problems for the biharmonic equation and the iterated Laplacian in a 3D-domain with an edge. *J. Math. Sci.*, **143**, 2936–2960.

Nazarov, S. A. & Sweers, G. (2007b) A hinged plate equation and iterated Dirichlet Laplace operator on domains with concave corners. *J. Differential Equations*, **233**, 151–180.

Rafetseder, K. & Zulehner, W. (2018) A decomposition result for Kirchhoff plate bending problems and a new discretization approach. *SIAM J. Numer. Anal.*, **56**, 1961–1986.

Sweers, G. (2009) A survey on boundary conditions for the biharmonic. *Complex Var. Elliptic Equ.*, **54**, 79–93.

Zhang, S. & Zhang, Z. (2008) Invalidity of decoupling a biharmonic equation to two Poisson equations on non-convex polygons. *Int. J. Numer. Anal. Model.*, **5**, 73–76.

Zulehner, W. (2015) The Ciarlet–Raviart method for biharmonic problems on general polygonal domains: mapping properties and preconditioning. *SIAM J. Numer. Anal.*, **53**, 984–1004.